Experimental Eye Research 262 (2026) 110737

Contents lists available at ScienceDirect

Experimental Eye Research

journal homepage: www.elsevier.com/locate/yexer

Research article

Bone marrow-*versus* adipose tissue-derived mesenchymal stem cells for corneal failure in an experimental model of limbal stem cell deficiency

Sara Galindo [a,b,c,d,1], Marina López-Paniagua [a,b,c,d,e,1], Ana de la Mata [a,b,c,f,g,1], José M. Herreras [a,b,c,e,h], Carmen García-Vázquez [a,3], Beatriz Marceñido [a,b,c], Esther Rey [a,b,4], Celia Higuera-Barón [a,5], Margarita Calonge [a,b,c,e,g,2], Teresa Nieto-Miguel [a,b,c,d,e,g,*,2]

[a] Grupo de Superficie Ocular, Instituto Universitario de Oftalmobiología Aplicada (IOBA), Universidad de Valladolid, Valladolid, Spain
[b] Centro de Investigación Biomédica en Red de Bioingeniería, Biomateriales y Nanomedicina (CIBER-BBN), Instituto de Salud Carlos III, Spain
[c] Centro en Red de Medicina Regenerativa y Terapia Celular de Castilla y León, Valladolid, Spain
[d] Departamento de Biología Celular, Genética, Histología y Farmacología, Universidad de Valladolid, Valladolid, Spain
[e] Redes de Investigación Cooperativa Orientadas a Resultados en Salud (RICORS) en Terapias Avanzadas (TERAV), Instituto de Salud Carlos III, Madrid, Spain
[f] Departamento de Pediatría, Inmunología, Obstetricia y Ginecología, Nutrición y Bromatología, Psiquiatría e Historia de la Ciencia, Universidad de Valladolid, Valladolid, Spain
[g] Unidad de Excelencia del Instituto de Oftalmobiología Aplicada (IOBA), Universidad de Valladolid, Valladolid, Spain
[h] Servicio de Oftalmología, Hospital Clínico Universitario de Valladolid, Valladolid, Spain

ARTICLE INFO

Keywords:
Cornea
Corneal epithelium
Limbus
Limbal stem cell deficiency
Mesenchymal stem cells
Regeneration
Stem cell transplantation

ABSTRACT

Ocular limbal stem cell deficiency (LSCD) occurs because of corneal epithelial stem cell destruction or dysfunction at the limbal niche. LSCD can cause corneal blindness, and the current therapy based on limbal stem cell transplantation is continuously improving. The aim of this work was to compare the safety and efficacy of human mesenchymal stem cells (hMSCs) derived from bone marrow (hBM-MSCs) and adipose tissue (hAT-MSCs) when transplanted to a rabbit model of LSCD. Both hMSC types expressed the corneal and limbal epithelial cell markers CK3, CK12, ZO-1, and ABCG2 under standard culture conditions. A few hBM-MSCs expressed CK7 and E-cadherin, while hAT-MSCs expressed more CK7 but no E-cadherin. The hMSCs were seeded onto amniotic membranes and transplanted onto the ocular surface of a LSCD rabbit model. Both hMSC types were well tolerated without immunosuppression and were primarily located in the superior limbal stroma eight weeks post-transplantation. The hBM-MSC–treated group showed less superficial neovascularization, while the hAT-MSC–treated group showed less conjunctival invasion and fewer corneal stromal blood vessels. Compared to the untreated LSCD group, both hMSC-treated groups had less corneal opacity, less corneal and limbal stromal inflammation, and more corneal epithelial layers that partially recovered the corneal and limbal epithelial markers CK3, CK15, and p63. Overall, transplantation of hBM-MSCs and hAT-MSCs in a rabbit LSCD model reduced the development of corneal opacity, neovascularization, inflammation, and partially restored corneal and limbal tissue structure and epithelial cell phenotypes. Therefore, both types of hMSCs could become valid alternatives for LSCD treatment.

* Corresponding author. Departamento de Biología Celular, Genética, Histología y Farmacología Facultad de Medicina, Universidad de Valladolid, Avenida Ramón y Cajal, 7, 47005, Valladolid, Spain.
E-mail address: teresa.nieto@uva.es (T. Nieto-Miguel).

[1] These authors contributed equally to this work and share first authorship.
[2] Co-senior authors.
[3] Current affiliation: Departamento de Cirugía, Oftalmología, Otorrinolaringología y Fisioterapia. Universidad de Valladolid, Valladolid, Spain.
[4] Current affiliation: Biobanco. Hospital Universitario de La Princesa, Instituto de Investigación Sanitaria del Hospital Universitario de La Princesa, Madrid, Spain.
[5] Current affiliation: VIVEbiotech, San Sebastián, Gipuzkoa, Spain.

https://doi.org/10.1016/j.exer.2025.110737
Received 7 July 2025; Received in revised form 27 September 2025; Accepted 6 November 2025
Available online 7 November 2025

List of abbreviations

ABCG2	ATP binding cassette subfamily G member 2
ARVO	Association for Research in Vision and Ophthalmology
AT	adipose tissue
AT-MSCs	adipose tissue-derived mesenchymal stem cells
BM	bone marrow
BM-MSCs	bone marrow-derived mesenchymal stem cells
BrdU	5′-bromo-2′-deoxyuridine
CLET	cultivated limbal epithelial cell transplantation
CK	cytokeratin
E-cad	E-cadherin
hAT-MSCs	human adipose tissue-derived mesenchymal stem cells
hBM-MSCs	human bone marrow-derived mesenchymal stem cells
LESCs	limbal epithelial stem cells
LSCD	limbal stem cell deficiency
MSCs	mesenchymal stem cells
PAS	periodic acid-Schiff
SPSS	Statistical Procedures for the Social Sciences
PBS	phosphate-buffered saline
ZO-1	zonula occludens-1

1. Introduction

Continuous regeneration of the corneal epithelium is vital to maintain the integrity and transparency of the cornea. The limbal epithelial stem cells (LESCs) are responsible for this renewal (Cotsarelis et al., 1989; Schermer et al., 1986). The loss or dysfunction of LESCs or their niche, causes the so-called "limbal stem cell deficiency" (LSCD) syndrome. This syndrome prevents the continuous regeneration of the corneal epithelium and is characterized by conjunctivalization and/or other signs of epithelial dysfunction, such as persistent or recurrent epithelial defects, with or without neovascularization, ocular surface inflammation, and scarring (Deng et al., 2019). These alterations ultimately lead to ocular surface inflammation, chronic pain, and ulceration, and can result in corneal blindness due to the loss of corneal transparency (Calonge et al., 2021; Dua et al., 2000). Cultivated limbal epithelial cell transplantation (CLET) is currently the treatment of choice for LSCD (Rama et al., 2010; Ramírez et al., 2015). However, the low availability of donors and the difficulty of culturing limbal epithelial cells make mesenchymal stem cells (MSCs) an encouraging alternative to this treatment.

The usefulness of MSCs in cell therapy and regenerative medicine is due to their potential to modulate the local environment, enabling activation of endogenous progenitor cells and secretion of trophic factors with immunomodulatory and anti-inflammatory properties. They also can migrate to injured tissues and have the potential for multipotent differentiation. This capacity allows the integration, proliferation, and differentiation of MSCs in damaged tissues (Ghiasi et al., 2021; Venkatakrishnan et al., 2022). Therefore, MSCs present at least four potential advantages over LESCs for treating LSCD: (1) they are readily obtained from several tissues types and can be acquired from living donors (Rohban and Pieber, 2017); (2) they can be cultured to clinical scales in a short period of time, thus, overcoming the limitations of LESCs (O'Callaghan and Daniels, 2011; Zhang et al., 2015); (3) they are not immunogenic and therefore immunosuppression is not necessary after allogeneic MSC transplantation; and (4) they can be cryopreserved without affecting their potency (Luetzkendorf et al., 2015).

Although there are many different MSC sources, bone marrow (BM) and adipose tissue (AT) are among the most commonly used for corneal regeneration. Isolated BM-MSCs can be transplanted by subconjunctival injection, or they can be cultured on amniotic membrane or fibrin and then transplanted to the ocular surface. Both injected and transplanted MSCs have immunomodulatory properties and improve repair of the ocular surface in mouse, rat, and rabbit LSCD models (Alió del Barrio et al., 2022; Calonge et al., 2021; Galindo et al., 2021; Nieto-Miguel et al., 2019). In fact, our research group has recently published the first evidence that human corneal epithelium, damaged by LSCD, was improved as efficiently by allogeneic BM-MSCs as by allogeneic CLET (Calonge et al., 2019). However, AT-derived MSCs (AT-MSCs) are more accessible, more cost-effective, and are a safer source of MSCs than BM (Strioga et al., 2012).

Delivery of AT-MSCs by topical administration, subconjunctival injection, or by transplantation on amniotic membranes or other substrata reduces clinical signs such as neovascularization, corneal opacity, and epithelial defects in rat and rabbit models of LSCD (Alió del Barrio et al., 2022; Espandar et al., 2014; Galindo et al., 2021, 2017; Holan et al., 2015; Lin et al., 2013; Zeppieri et al., 2013). Additionally, authors have reported that AT-MSCs express basal levels of some corneal epithelial markers (Martínez-Conesa et al., 2012; Nieto-Miguel et al., 2013). However, to date, there are no studies that compare the safety and the clinical, histological, and phenotypic efficacies of corneal regeneration based on human BM- and AT-derived MSCs. Obtaining this information using in vivo models is an essential step for translating results in experimental models of LSCD into clinical trials in LSCD patients. Therefore, in the absence of this critical information based on human MSCs (hMSCs), the present work provides a comparison of both the safety and efficacy of hAT-MSC versus hBM-MSC transplantation for regeneration of corneal epithelium in a rabbit model of LSCD. Thus, this study establishes the basis for translation of this treatment to patients suffering corneal failure due to LSCD.

2. Materials and methods

Ethics approval

The study was conducted in accordance with the Declaration of Helsinki, and the protocol was approved by the IOBA Research Committee and the Ethics Committee of the University Clinical Hospital of Valladolid, Spain (PI 16–442: June 17, 2016; PI-18-1116: October 18, 2018). The animal study protocol was approved by the Animal Care Committees of the University of Valladolid and the Regional Government of Castilla y León, Spain (1004476: July 6, 2016). The study followed the ARRIVE guidelines for reporting animal research (Percie du Sert et al., 2020). All procedures followed the standards of Association for Research in Vision and Ophthalmology (ARVO) as provided in the Statement for the Use of Animals in Ophthalmic and Visual Research.

2.1. Isolation and culture of hMSCs

Commercial hBM-MSCs (ATCC® PCS-500-012™, ATCC, Manassas, VA, USA) and non-commercial subcutaneous hAT-MSCs were used. Subcutaneous human AT was obtained by liposuction procedures in a medical aesthetic clinic after obtaining each patient's written informed consents. The privacy rights of human subjects were observed. Cells were isolated using the procedures described previously (Galindo et al., 2017), and characterized (Nieto-Miguel et al., 2013) in accordance with the International Society for Cellular Therapy (ISCT) position statement (Dominici et al., 2006).

2.2. hMSC labeling and seeding on amniotic membrane

Before transplanting, hBM-MSCs and hAT-MSCs were incubated with 10 mM 5′-bromo-2′-deoxyuridine (BrdU, BD Biosciences, San Jose, CA, USA) in culture medium for 24 h at 37 °C. Human amniotic membranes were provided by the Center for Hemotherapy and Hemodonation of Castilla y León (Valladolid, Spain), and processed as previously

described (Galindo et al., 2017). Two hundred and fifty thousand P3-5 hBM-MSCs or hAT-MSCs were seeded on each de-epithelialized amniotic membrane piece.

2.3. Development of a total LSCD model in rabbits and clinical evaluation of the ocular surface

The care of animals was in accordance with institutional guidelines. A total LSCD model was developed in adult female New Zealand white rabbits (*Oryctolagus cuniculus*). After n-heptanol (Sigma-Aldrich, St. Louis, MO, USA) denudation of the corneal surface, a 360° surgical limbal peritomy was performed (Galindo et al., 2017). The eyes were divided into three groups: Group 1, LSCD without treatment (n = 9); Group 2, LSCD treated with hBM-MSCs (n = 9); and Group 3, LSCD treated with hAT-MSCs (n = 9). Contralateral healthy eyes were used as the control group.

Prior to surgery, the rabbits were anesthetized by intramuscular injection of 50 mg/kg ketamine (Imalgene 1000, Merial, Lyon, France) and 7 mg/kg xylazine (Rompun, Bayer, Leverkusen, Germany), complemented with topical ophthalmic anesthesia (1 mg/mL tetracaine and 4 mg/mL oxybuprocaine, Colicursi, Alcon, Barcelona, Spain). Systemic analgesia (0.04 mg/kg buprenorphine, Buprex, Indivior, Bristol, UK) was administered daily for 4 days after surgery. Topical anti-inflammatory and antibiotic agents including Maxitrol (3500 IU/mL neomycin; 6000 IU/mL polymyxin B; and 1 mg/mL dexamethasone, Alcon), Tobrex (3 mg/g tobramycin ointment, Alcon), and systemic antibiotic (5 mg/kg enrofloxacin, Alsir, Esteve, Barcelona, Spain) were administered daily for 5 days.

Conjunctival invasion, corneal neovascularization, opacification, and epithelial defects stained with sodium fluorescein (Colircusi Fluotest, Alcon) were clinically examined on a weekly basis by slit lamp biomicroscopy (Kowa SL-15, Kowa Medicals, Tokyo, Japan). Clinical signs were assessed by two different researchers using a score system (Wan et al., 2011) (Fig. 1). The cornea was first divided into five areas that were scored independently, and the final score for each cornea was calculated as the mean value for each clinical sign evaluated. In addition, epithelial defect areas were measured by the image-processing program ImageJ (http://rsb.info.nih.gov/ij/).

2.4. Transplantation of hMSCs

Three weeks after injury, the hMSC-loaded amniotic membranes were transplanted onto the ocular surface of 18 rabbits. The membranes covered the corneal and limbal areas where they were sutured to the sclera. Prior to transplantation, the rabbits were properly administered with anesthesia and analgesics following the protocol described above. In eyes where conjunctival invasion occurred (three rabbits from the hBM-MSC group and two rabbits from the hAT-MSC group), the invading tissue was removed before the hMSC transplantation.

After transplantation, the eyelids were closed for two weeks with a partial tarsorrhaphy. Triamcinolone (40 mg, Trigon Depot, Bristol-Myers Squibb, Madrid, Spain) was administered by transeptal injection. Systemic analgesics (0.02 mg/kg buprenorphine) were administered 8 h after transplantation and daily for the next 4 days. Topical anti-

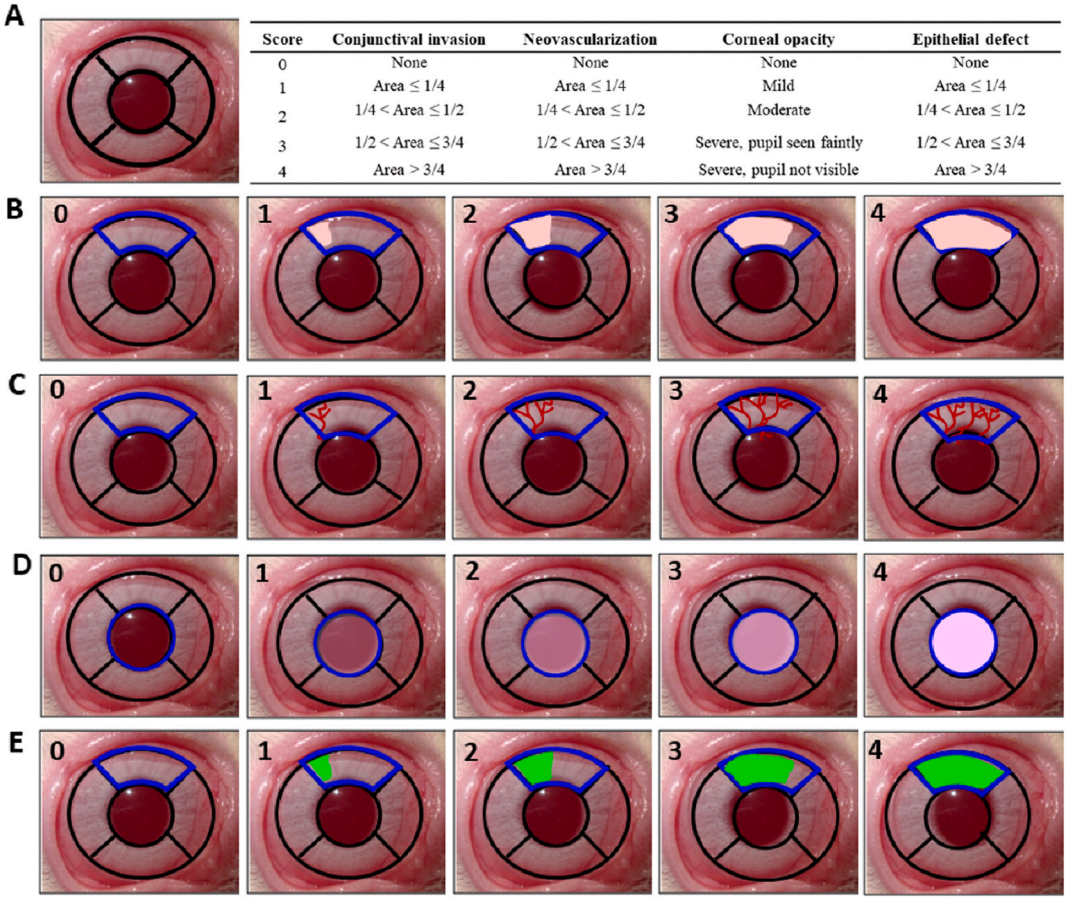

Score	Conjunctival invasion	Neovascularization	Corneal opacity	Epithelial defect
0	None	None	None	None
1	Area ≤ 1/4	Area ≤ 1/4	Mild	Area ≤ 1/4
2	1/4 < Area ≤ 1/2	1/4 < Area ≤ 1/2	Moderate	1/4 < Area ≤ 1/2
3	1/2 < Area ≤ 3/4	1/2 < Area ≤ 3/4	Severe, pupil seen faintly	1/2 < Area ≤ 3/4
4	Area > 3/4	Area > 3/4	Severe, pupil not visible	Area > 3/4

Fig. 1. Score system to evaluate clinical signs. The cornea was first divided into five areas that were scored independently following the score system used to evaluate the clinical signs (A). Conjunctival invasion (B), neovascularization (C), corneal opacity (D), and epithelial defects stained with sodium fluorescein (E) were assessed by two different researchers. Panels B, C, and E represent the rating scale of the superior area for conjunctival invasion (B), neovascularization (C), and epithelial defects (E). Panel D represents the rating scale of the central area for corneal opacity. The final score for each clinical sign in each cornea was calculated as the mean value of the five areas.

Table 1
Measure of inflammation.

Assigned value	Presence of stromal lymphocytes
1	Very few dispersed lymphocytes
2	Few dispersed lymphocytes
3	Few dispersed lymphocytes and a few lymphocyte aggregates
4	Many dispersed lymphocytes
5	Many lymphocytes forming cell aggregates

The presence of stromal lymphocytes was semi-quantitatively assessed and rated as mild (1–2), moderate (> 2–4), or severe (> 4–5) according to the following score system.

inflammatory and antibiotics and systemic antibiotics were administered daily for 10 days.

Eight weeks after transplantation, the animals were euthanized by intravenous injection of 200 mg/kg pentobarbital sodium (Dolethal, Vetoquinol, Lure, France). Corneo-scleral buttons were collected and fixed in 4 % paraformaldehyde at 4 °C for 4 h (Santa Cruz Biotechnology, Dallas, TX, USA) for histopathology and immunophenotypic analysis.

2.5. Histopathology analysis

Fixed corneo-scleral buttons were cut along the sagittal plane of the central cornea. Nasal portions of the corneo-scleral samples were washed, processed using the HISTO-PRO 300 vacuum tissue processor (HISTO-Line Laboratories, Pantigliate, Italy), and embedded in paraffin. Subsequently, tissue sections (5 μm) were deparaffinized, rehydrated, and stained with periodic acid-Schiff-hematoxylin following a standard protocol. Each section included the superior conjunctiva, superior limbus, cornea, inferior limbus, and inferior conjunctiva.

The number of epithelial layers was counted in each sample, and the percentage of samples containing blood vessels in the corneal stroma was calculated. As a measure of inflammation, the presence of stromal lymphocytes was semi-quantitatively assessed and rated as mild (1–2), moderate (> 2–4), or severe (>4–5) according to a score system (Table 1). The percentages of the samples that showed mild, moderate, and severe inflammation were calculated. In addition, the presence of goblet cells was analyzed as a sign of conjunctival in-growth. For each rabbit, goblet cells in the limbal and corneal epithelia were recorded as present or absent, and the percentage of animals with goblet cells in the limbal and/or corneal epithelium was then calculated. Histopathological analysis was performed using an optical microscope (DM400B, Leica Biosystems, Wetzlar, Germany).

2.6. Immunophenotypic analysis and hMSC localization in histological sections

P3-4 hBM-MSCs and hAT-MSCs from 3 different donors in each case were seeded in Permanox multichambers (Life Technologies, Waltham, MA, USA) and fixed with cold methanol in order to analyze the expression of epithelial cell markers in basal conditions by hMSCs. Histological sections from the ocular surface of the transplanted rabbits were deparaffinized and rehydrated. For BrdU detection, the DNA was denatured by incubating the samples in 2 N HCl for 30 min at room temperature, followed by three washes in 0.1 M sodium borate (pH 8.5) for 10 min at room temperature. Immunophenotypic analysis of all histological sections was begun by antigen retrieval with 0.1 % trypsin. The samples were then washed with phosphate-buffered saline (PBS; Life Technologies), permeabilized with 0.3 % Triton X-100, and blocked with PBS containing 5 % donkey serum (Sigma-Aldrich) for 1 h at room temperature. Then, they were incubated overnight at 4 °C with cell-specific primary antibodies (Table 2) (Chen et al., 2004; Galindo et al., 2017).

Subsequently, the samples were incubated with the secondary antibody (Table 2) in PBS for 1 h in darkness at room temperature. To avoid tissue autofluorescence, the sections were then incubated with a TrueView Autofluorescence Quenching Kit (Vector Laboratories, Newark, CA, United States). Finally, cell nuclei were counterstained with Hoechst (Sigma-Aldrich), and the samples were mounted with Vectashield Vibrance mounting medium (Vector Laboratories). All samples were imaged using an inverted fluorescence microscope (DM6000B, Leica Biosystems). Negative controls were prepared by omitting the use of primary antibody. For the hMSCs cultured on Permanox multichambers, the percentage of positive cells was calculated by counting the total number of cells and positive cells in 5 random different areas from each cell donor using the image-processing program ImageJ. The fluorescence of every marker in the inferior and superior limbus and the inferior, central, and superior cornea was evaluated in two sections per rabbit, from 5 different rabbits in each experimental group.

For hMSC localization, BrdU-positive cells were semi-quantitatively analyzed in the epithelium and stroma of the superior and inferior limbus, and superior, central, and inferior cornea. The data were semi-quantitatively assigned into four groups: (−) no detectable BrdU-positive cells, (+) a few isolated BrdU-positive cells, (++) a moderate number of BrdU-positive cells, and (+++) an elevated number of BrdU-positive cells.

2.7. Statistical analysis

Statistical analyses were performed using the Statistical Procedures for the Social Sciences (SPSS 26.0, IBM Corporation, Armonk, NY, United States). Two-sided p-values ≤ 0.05 were considered statistically significant. Student's t-test was used for analysis of ocular surface markers in MSCs. For analysis of qualitative variables, the Kruskal-Wallis test for more than two groups or the Mann-Whitney *U* test for two groups were used. The Friedman test for more than two groups or the Wilcoxon test for two groups were used to compare values over time. For histopathology analysis, statistical significance of the number of epithelial layers was determined by one-way factorial ANOVA. The post-

Table 2
Antibodies.

Antibody	Host	Specificity	Clone	Source	Dilution
Anti-CK3	Mouse	Corneal epithelial cells	AE5	MP Biomedicals	1/50
Anti-CK12	Rabbit	Corneal epithelial cells		Santa Cruz Biotechnology	1/50
Anti-E-cadherin	Mouse	Corneal epithelial cells	36	BD Biosciences	1/100
Anti-ZO-1	Rabbit	Corneal epithelial cells		Thermo Fisher	1/50
Anti-ABCG2	Mouse	Limbal epithelial stem cells	BXP-21	Merck	1/20
Anti-CK15	Mouse	Limbal epithelial stem cells	LHK15	Merck	1/50
Anti-p63α	Rabbit	Limbal epithelial stem cells		Cell Signaling Technology	1/50
Anti-p63	Mouse	Limbal epithelial stem cells	4A4	Abcam	1/50
Anti CK7	Mouse	Conjunctival epithelial cells	OV-TL12/30	Vector Laboratories	1/50
Anti-BrdU	Mouse	BrdU-labeled MSCs	NB500-235	Novus Biological	1/200
Anti-rabbit IgG Alexa fluor 488	Donkey	Secondary antibody		Thermo Fisher	1/300
Anti-mouse IgG Alexa fluor 488	Donkey	Secondary antibody		Thermo Fisher	1/200
Anti-sheep IgG Alexa fluor 594	Donkey	Secondary antibody		Thermo Fisher	1/200

hoc Tuckey test was used for pairwise contrasts. The statistical significance of the percentage of samples with blood vessels in corneal stroma, the percentage of samples with inflammation, and the BrdU-positive cells were analyzed by chi-square tests (χ^2 test). All values were expressed as means ± standard error of the means.

3. Results

3.1. Expression of epithelial cell markers by hMSCs

At 24 h of culture on Permanox plates, both hBM-MSCs and hAT-MSCs in P3-4 expressed corneal epithelial cell markers such as CK3, CK12, and ZO-1 (Fig. 2A and B). While there was no difference in the expression of CK12 and ZO-1 between the hBM-MSCs and hAT-MSCs ($p > 0.05$ each), a significantly higher percentage of hAT-MSCs expressed CK3 compared to hBM-MSCs ($p < 0.05$, Fig. 2B). In addition, because hBM-MSCs from one of the three donors did not express any detectable CK3, there were donor-to-donor variations. The corneal epithelial cell marker E-cad was expressed by only one hBM-MSC donor, while none of the hAT-MSCs expressed it. Thus for E-cad, the percentage of positive hBM-MSCs was significantly greater than hAT-MSCs ($p < 0.05$, Fig. 2A and B).

All of the hBM-MSC and hAT-MSC donors expressed the limbal epithelial cell marker ABCG2, but were negative for the transcription factor p63α (Fig. 2A and B). CK15, also a limbal epithelial cell marker, was present in only a few cells from one of the hBM-MSC donors, while none of the hAT-MSCs expressed it (Fig. 2A and B). The conjunctival epithelial cell marker CK7 was expressed by 50 % of hAT-MSCs and 20 % of hBM-MSCs ($p < 0.01$, Fig. 2A and B) without differences between the donors.

3.2. Clinical evaluation

Because both hBM and hAT cell types were well tolerated in the ocular surface of the rabbits, there was no need for immunosuppression. Immediately after the corneal injury, the epithelial defect scores and defect areas were high in all three groups (Fig. 3A). For each group, both the defect scores and the areas tended to decrease during the first three weeks after injury, without differences among the three groups (Fig. 3A and B).

Beginning at 2–3 weeks after LSCD induction, conjunctival invasion developed in 4 rabbits of the untreated control group. In the hBM-MSC group it developed in 3 rabbits, and in the hAT-MSC group, it occurred in only 2 rabbits. At 3–5 weeks after transplantation (6–8 weeks after LSCD induction), conjunctival invasion in the hAT-MSC–treated group was significantly less than in the untreated control group (Fig. 3A). While the conjunctival invasion of hBM-MSC–treated eyes were also lower than in the control eyes, the differences at each of the measured times was not statistically significant. There were no differences in conjunctival invasion between hAT-MSC and hBM-MSC treatment groups.

Corneal neovascularization increased in all three groups during the first three weeks following induction of LSCD (Fig. 3A). At 3–5 weeks after transplantation (6–8 weeks after LSCD induction), neovascularization in the hBM-MSC–treated group was significantly less than in the untreated control group. However, there were no differences in neovascularization between the hAT-MSC–treated group and the untreated control group, nor between the hBM-MSC- and hAT-MSC–treated groups.

Corneal opacity increased in all three groups during the first 3 weeks following the induction of LSCD (Fig. 3A). At 3–6 weeks after transplantation (6–9 weeks after LSCD induction), the opacity was significantly lower in the hBM-MSC and the hAT-MSC–treated groups than in the untreated group (Fig. 3A). For the hAT-MSC–treated group, the reduction in opacity lasted until 7 weeks after transplantation (10 weeks after LSCD induction, Fig. 3A).

3.3. Histopathology analysis

The number of epithelial cell layers in the superior limbus and cornea was significantly lower ($p < 0.01$) in rabbits in which LSCD was induced (superior limbus 4.5 ± 0.4; cornea 2.7 ± 0.3) than in rabbits of the healthy control group (superior limbus 6.5 ± 0.2; cornea 4.4 ± 0.1)

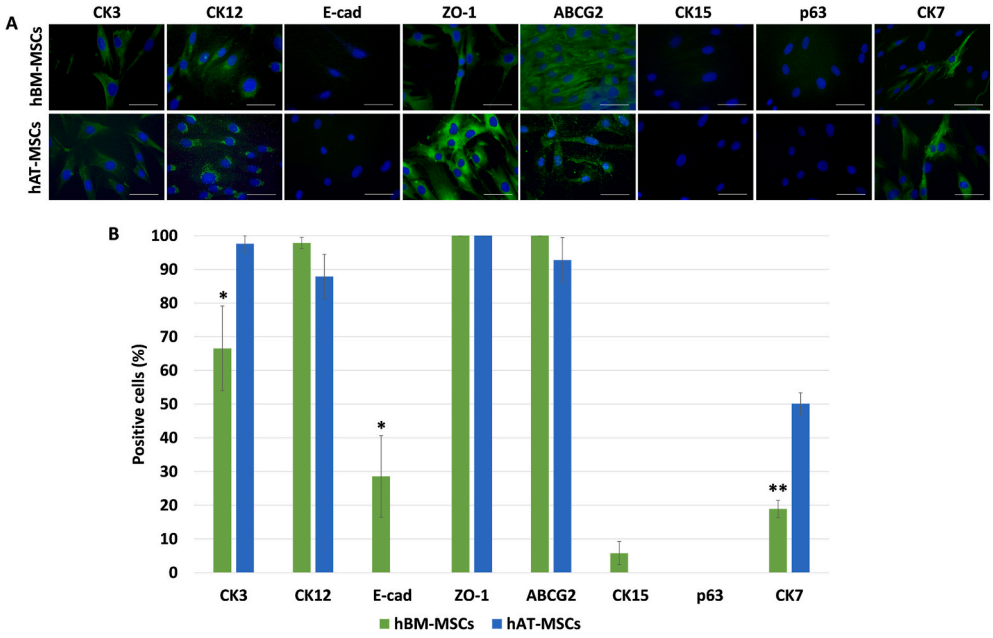

Fig. 2. Expression of the ocular surface cell markers CK3, CK12, E-cad, ZO-1, ABCG2, CK15, p63α, and CK7 by P3-4 human bone marrow-derived mesenchymal stem cells (hBM-MSCs) and human adipose tissue-derived mesenchymal stem cells (hAT-MSCs) cultured on Permanox plates for 24 h. **A** Representative images from hBM-MSCs and hAT-MSCs showing ocular surface cell marker expression (in green) and nuclei (in blue). Scale bar = 50 μm. **B** Percentage of positive cells for each cell marker. Data are expressed as mean ± standard error of the mean (SEM) from 15 samples, 5 random different areas from each of the 3 cell donors. *$p < 0.05$; **$p < 0.01$. (For interpretation of the references to color in this figure legend, the reader is referred to the Web version of this article.)

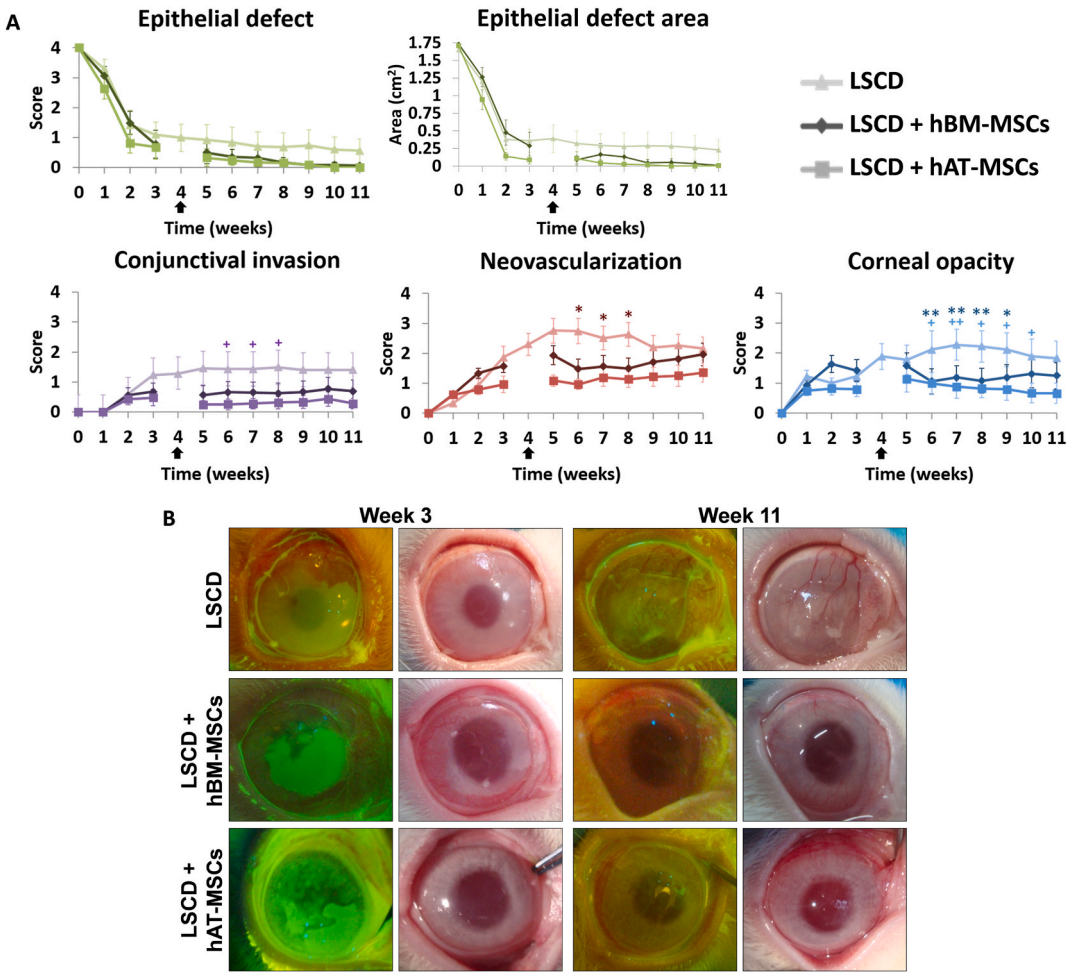

Fig. 3. Clinical sign evaluation in the rabbit limbal stem cell deficiency (LSCD) model of untreated eyes and eyes treated with either human bone marrow-derived mesenchymal stem cells (hBM-MSCs) or human adipose tissue-derived mesenchymal stem cells (hAT-MSCs). **A** Evolution of corneal epithelial defect score, corneal epithelial defect area, conjunctival invasion, neovascularization, and corneal opacity. Data are expressed as mean ± standard error of the mean (SEM) from 9 rabbits. The arrows indicate the week when it was not possible to assess the ocular surface of the treated rabbits (week 4) because the eyelid remained closed by tarsorrhaphy to protect the cell implant. **B** Representative images from the untreated LSCD model, hBM-MSC–treated group, and hAT-MSC–treated group. The first and third columns show corneal epithelial defects stained green with sodium fluorescein. The second and fourth columns show conjunctival invasion, neovascularization, and corneal opacity. Data for week 0 were acquired immediately after the injury. Data for week 3 were acquired before transplantation. *Comparison between untreated LSCD and hBM-MSC–treated groups: *$p < 0.05$; **$p < 0.01$. $^{+}$Comparison between untreated LSCD and hAT-MSC–treated groups: $^{+}p < 0.05$; $^{++}p < 0.01$. (For interpretation of the references to color in this figure legend, the reader is referred to the Web version of this article.)

(Fig. 4A and B). On the other hand, the number of corneal epithelial cell layers significantly increased when rabbits with LSCD were treated with either hBM-MSCs (4.0 ± 0.2, $p < 0.01$) or hAT-MSCs (4.3 ± 0.11, $p < 0.01$). There were no significant differences between the rabbits treated with hBM-MSCs or hAT-MSCs (Fig. 4B). There were also no significant differences among the control, LSCD, LSCD + hBM-MSC, and LSCD + hAT-MSC groups in the number of epithelial cell layers in the inferior limbus (Fig. 4B).

The percentage of tissue samples with blood vessels in the corneal stroma was significantly higher ($p < 0.01$) in the untreated LSCD group (63.0 %) than in the healthy control group, which had no blood vessels in the stroma (Fig. 4C). In addition, the percentage of tissue samples with corneal stromal blood vessels was lower in LSCD + hBM-MSC (48.1 %) and LSCD + hAT-MSC (18.5 %) groups than in rabbits with untreated LSCD. However, the difference was significant between untreated LSCD and LSCD + hAT-MSC groups ($p < 0.01$) (Fig. 4C) but not between the LSCD and the LSCD + hBM-MSC groups (Fig. 4C).

There were no significant differences in the superior and inferior conjunctival area between the presence of lymphocytes in untreated LSCD eyes and eyes treated with either hBM-MSCs or hAT-MSCs (Fig. 4A–D). In the superior limbus, 63.0 % of the untreated LSCD eyes had mild inflammation and 37.0 % had moderate inflammation. In contrast, 88.5 % of the eyes treated with hBM-MSCs had mild superior limbal inflammation and 11.5 % had moderate inflammation ($p < 0.05$ vs untreated LSCD, Fig. 4A–D). For the inferior limbus, 59.5 % of the untreated LSCD eyes had mild inflammation and 40.7 % had moderate inflammation. For LSCD + hBM-MSC–treated eyes, 84.6 % had mild inflammation and 15.4 % had moderate inflammation ($p = 0.076$ vs untreated LSCD eyes). In contrast, 96.3 % of eyes treated with hAT-MSCs had mild inferior limbal inflammation and 3.7 % had moderate inflammation ($p < 0.01$ vs untreated LSCD, Fig. 4A–D). There were no significant differences between LSCD + hBM-MSC–treated and the LSCD + hAT-MSC–treated eyes ($p > 0.05$, Fig. 4D).

Lymphocytes were not detected in the corneal stroma of healthy eyes; however, they were evident in the corneal stromas of the LSCD, LSCD + hBM-MSC–, and LSCD + hAT-MSC–treated eyes (Fig. 4A). In the cornea, 66.7 % of the untreated LSCD eyes had mild inflammation, 29.6 % had moderate inflammation, and 3.7 % had severe inflammation. For LSCD + hBM-MSC–treated eyes, 92.6 % had mild inflammation and 7.4 % had moderate inflammation ($p = 0.056$ vs untreated LSCD eyes). For LSCD + hAT-MSC–treated eyes, 100 % had mild inflammation ($p < 0.01$ vs untreated LSCD eyes, Fig. 4A–D).

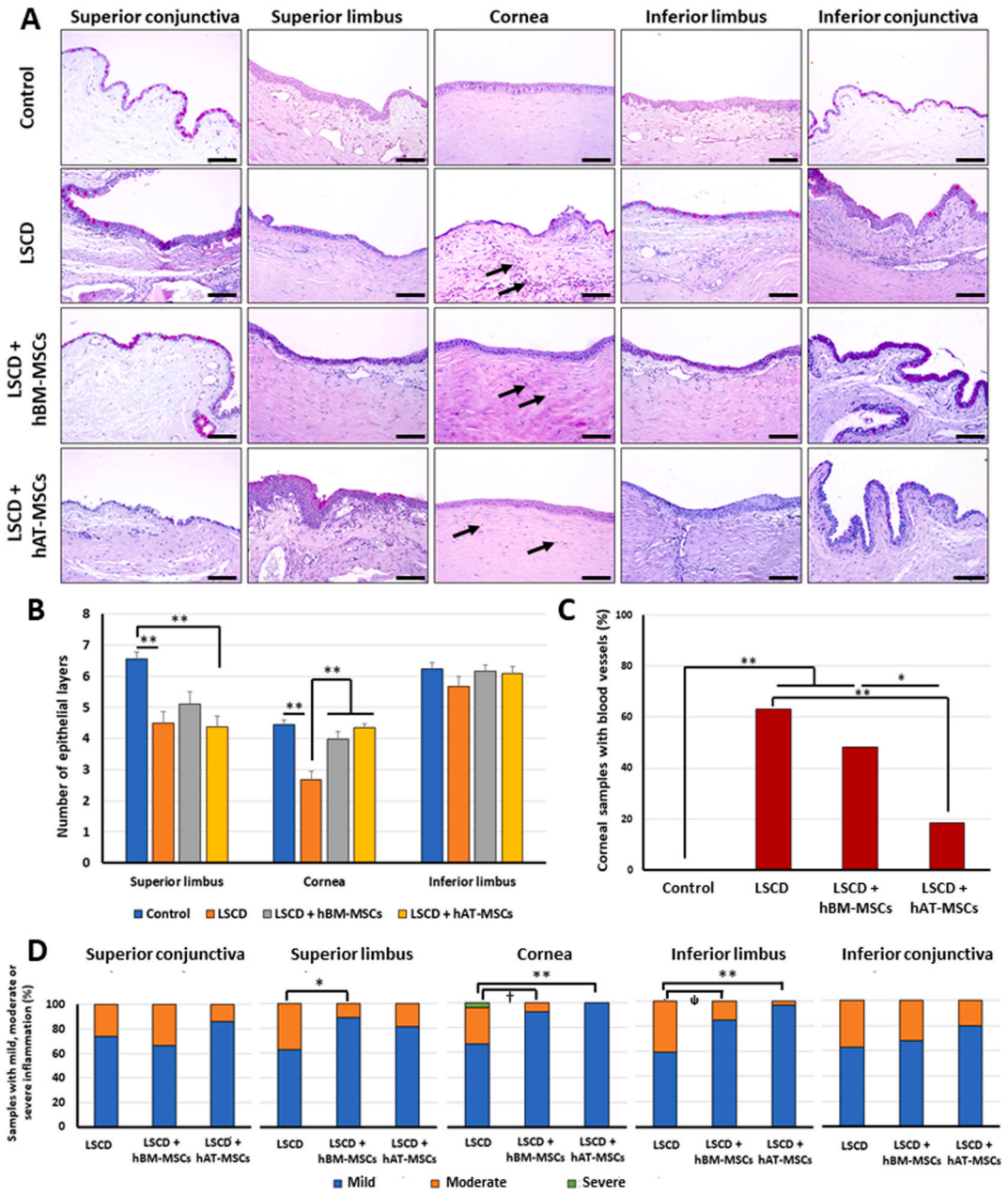

Fig. 4. Histopathology analysis performed at 11 weeks after LSCD induction (8 weeks after hBM-MSC or hAT-MSC transplantation). **A** Representative images of the histopathology analysis (periodic acid-Schiff-hematoxylin staining) of the superior conjunctiva, superior limbus, cornea, inferior limbus, and inferior conjunctiva in healthy control eyes (control), limbal stem cell deficiency model (LSCD), hBM-MSC–treated (LSCD + hBM-MSCs) and hAT-MSC–treated (LSCD + hAT-MSCs) eyes. Goblet cells were stained with fuchsia color. Scale bar = 200 μm. Black arrows: lymphocytes. **B** Number of epithelial cell layers. Data are expressed as mean ± standard error of the mean (SEM) from 12 samples in the healthy control group (6 eyes, 2 tissue levels per eye), and 27 samples (9 eyes, 3 tissue levels per eye) in each of the untreated LSCD, LSCD + hBM-MSC, and LSCD + hAT-MSC groups. **C** Percentage of eyes with stromal corneal blood vessels in 6 corneas from the control group and 9 corneas from each of the LSCD, LSCD + hBM-MSC, and LSCD + hAT-MSC groups. **D** Percentage of samples with mild, moderate, or severe inflammation as indicated by the presence of stromal lymphocytes. Nine corneas from each group were evaluated. Data represent significant differences in the eyes with mild, moderate, and severe infiltration. †$p = 0.056$; φ $p = 0.076$; *$p < 0.05$; **$p < 0.01$. hBM-MSCs: human bone marrow-derived mesenchymal stem cells; hAT-MSCs: human adipose tissue-derived mesenchymal stem cells. (For interpretation of the references to color in this figure legend, the reader is referred to the Web version of this article.)

Goblet cells were present in both the corneal and limbal epithelia of rabbits from the three experimental groups while they were not present in the corneal epithelium of healthy rabbit eyes. The percentage of rabbits with goblet cells in the limbal and/or corneal epithelium was similar in the untreated LSCD group and the LSCD + hBM-MSC group (66.7 %), and lower in the LSCD + hAT-MSC group (55.6 %) (Fig. 4A).

3.4. Immunophenotypic analysis and hMSC localization in histological sections

The expressions of specific corneal (CK3 and E-cad (Fig. 5)) and limbal (CK15 and p63 (Figs. 6 and 7)) epithelial markers were assessed. CK3 was expressed in all corneal epithelial cell layers and in the superficial cell layers of the limbus in the healthy control eyes (Fig. 5A). Expression decreased in the LSCD model compared to the healthy

control eyes in all the tissue areas (Fig. 5A). However, it increased in the cornea of both hBM-MSC– and hAT-MSC–treated eyes, showing a similar staining at 8 weeks after transplantation (11 weeks after LSCD induction).

The expression of E-cad (Fig. 5B) was not reduced in the LSCD model compared to the healthy control eyes, where it was expressed in all of the corneal epithelial cell layers and in the upper cell layers of the limbus. Thus for E-cad, no changes were evident between the healthy control tissues and the tissues from the LSCD model or either of the hMSC–treated eyes (Fig. 5B).

In LSCD eyes, loss of CK15 expression was evident in both the superior and inferior limbus (Fig. 6). At 8 weeks after transplantation with hBM- or hAT-MSCs, CK15 expression had recovered in both limbuses, though for both treatments the improvement was greater in the superior limbus (Fig. 6). There were no differences in the outcomes between hBM- and hAT-MSC-treated eyes.

Expression of p63 was reduced in the superior and inferior limbus following LSCD (Fig. 7). Following both hBM- and hAT-MSC transplantation, the p63 expression increased in both limbuses (Fig. 7), where the distribution became similar to that in healthy control eyes. No discernible differences were observed between the expression of p63 in hBM- and hAT-MSC–treated eyes. Expression of p63 in the cornea was not detected in healthy control eyes or in eyes treated with hMSC transplants.

The number and location of BrdU-labeled hBM-MSCs and hAT-MSCs were recorded in the epithelium and stroma of the limbus and cornea (Fig. 8A). More than 40 % of the samples contained only a few isolated BrdU-positive cells in the epithelium of the superior limbus and the superior and central cornea of both hBM-MSC– and hAT-MSC–treated eyes. For the inferior corneal and inferior limbal epithelia, BrdU-positive cells were absent in more than 50 % of the samples. Among the epithelial BrdU-containing cells in the hBM-MSC– and hAT-MSC–eyes, between 10 and 20 % expressed a moderate amount staining (Fig. 8B). There were no apparent differences in the percent of BrdU labeling between the hBM-MSCs and hAT-MSCs in the corneal or limbal epithelia.

There were no differences in the presence of BrdU-labeled hBM-MSCs and hAT-MSCs in the stromas of the superior and inferior limbus and the inferior cornea (Fig. 8). In the stroma of the superior limbus, 43.8 % and 36.8 % of the samples presented a moderate number of BrdU-labeled hBM-MSCs and hAT-MSCs, respectively.

In the superior corneal stroma, 64.7 % of the samples from LSCD eyes treated with hBM-MSC–transplants had BrdU-positive cells; while for hAT-MSC–treated eyes, 95 % of the samples were positively stained. Among these, 75 % had a few isolated stained cells, 20 % had a moderate number of stained cells, and 0 % had an elevated number of stained cells. For the central corneal stroma, BrdU-positive cells were present in the 35.3 % of the samples from hBM-MSC–treated eyes, while for hAT-MSC–treated eyes, 68.4 % had BrdU staining (Fig. 8; $p < 0.05$).

4. Discussion

Human MSCs are now widely studied as cell therapy candidates for the treatment of ocular surface pathologies and are showing very promising results. However, more information is needed to choose the most appropriate source of cells based on their capabilities and clinical targets. Thus, the expression of ocular surface markers by cultured hBM-MSCs and hAT-MSCs was compared and then, in an experimental model of rabbit LSCD, we examined the safety and efficacy of transplanted hBM-MSC– and hAT-MSC–loaded human amniotic membranes to restore the ocular surface cellular structure, tissue organization, and cell phenotypes to that of healthy control eyes.

In the current study, both hBM-MSCs and hAT-MSCs expressed corneal epithelial markers such as CK3, CK12, and ZO-1 when cultured on plastic. The expression of CK3 and CK12 in hBM-MSCs (Nieto-Nicolau et al., 2020), hAT-MSCs (Martínez-Conesa et al., 2012; Nieto-Miguel et al., 2013), and rabbit BM-MSCs (Reinshagen et al., 2011) was previously described by us and other authors. In the present work, CK3 expression was significantly higher in hAT-MSCs than in hBM-MSCs. However, the expression of CK12 was similar for both types of MSCs. Nieto-Nicolau et al. found that CK3 mRNA expression was higher in hAT-MSCs, while CK12 mRNA expression was higher in hBM-MSCs (Nieto-Nicolau et al., 2020). In contrast, Sikora et al. reported the absence or very low mRNA expression levels of CK3 and CK12 in commercially available hAT-MSCs from a single donor (Sikora et al., 2019). Our results support the variability in marker expression levels among cells isolated from different donors. For instance, only 30 % of the hBM-MSCs in culture exhibited E-cad expression, while none of the hAT-MSCs expressed this marker. Bandeira et al. also found that E-cad was not expressed in hAT-MSCs (Bandeira et al., 2020).

The LESC marker ABCG2 was expressed at similar levels in both hBM-MSCs and hAT-MSCs cultured on plastic. However, the LESC markers CK15 and p63α were either undetectable or present at very low levels in both types of hMSCs. Dos Santos et al. also observed similar expression of ABCG2 mRNA in hBM-MSCs and hAT-MSCs (Dos Santos et al., 2019), and Martinez-Conesa et al. reported ABCG2 mRNA expression by hAT-MSCs (Martínez-Conesa et al., 2012). Based on either immunohistochemistry or mRNA analyses, other authors have reported the absence of p63 and low levels of CK15 in both hBM-MSCs and hAT-MSCs cultured on plastic (Bandeira et al., 2020; Martínez-Conesa et al., 2012; Nieto-Nicolau et al., 2020; Sikora et al., 2019).

Collectively, our results demonstrate that both types of hMSCs express specific markers of ocular surface, suggesting that hMSCs could act to repair the ocular surface when transplanted to the damaged cornea.

To compare the potential for repairing damaged ocular surfaces, hBM-MSCs and hAT-MSCs cultured on human amniotic membranes were transplanted to the ocular surface of our rabbit experimental model of LSCD. The validity of this model is supported by significant histological changes in the cornea and limbus. Compared to the healthy controls, untreated LSCD eyes showed (1) fewer epithelial layers in the limbus and cornea, (2) increased corneal stromal neovascularization, and (3) greater lymphocyte infiltration in the cornea.

As previously reported by us and others (Espandar et al., 2014; Galindo et al., 2017; Lee et al., 2014; Lin et al., 2013; Ma et al., 2006; Roddy et al., 2011; Rohaina et al., 2014; Yun et al., 2017; Zeppieri et al., 2013), the transplanted hBM-MSC– and hAT-MSC–coated amniotic membranes were well tolerated without the need for immunosuppression during the 8-week period following transplantation.

Both types of hMSCs induced a significant reduction in corneal opacity between 3 and 6 weeks after transplantation compared to the untreated group. In eyes with hBM-MSC transplants, neovascularization was reduced at 3–5 weeks after transplantation, but not in eyes transplanted with hAT-MSCs. During that same period, conjunctival overgrowth of the cornea was reduced in eyes receiving the hAT-MSCs transplants, but not in eyes transplanted with hBM-MSCs. These results for neovascularization and opacity are similar to those reported by our group and others after transplantation of MSCs cultured on amniotic membranes (Galindo et al., 2017; Jiang et al., 2010; Ma et al., 2006; Pınarlı et al., 2014; Rohaina et al., 2014). Although there were no statistically significant differences in clinical outcomes between the two hMSC types, in comparison with the untreated LSCD group, only hBM-MSCs significantly reduced corneal neovascularization, while only hAT-MSCs significantly reduced conjunctival overgrowth of the cornea. In contrast, we found that the percentage of samples with corneal stromal blood vessels was significantly lower only in the hAT-MSCs-treated group compared to the untreated animals. This discordance between clinical and histopathologic findings may be explained by the fact that the neovascularization detected during clinical follow-up was more superficial, whereas the blood vessels observed histologically were deeper and therefore more difficult to detect in vivo. Overall, both cell types contributed to the reduction of corneal neovascularization.

Although we did not find clinically significant differences in epithelial defects among the different study groups, in LSCD rabbits

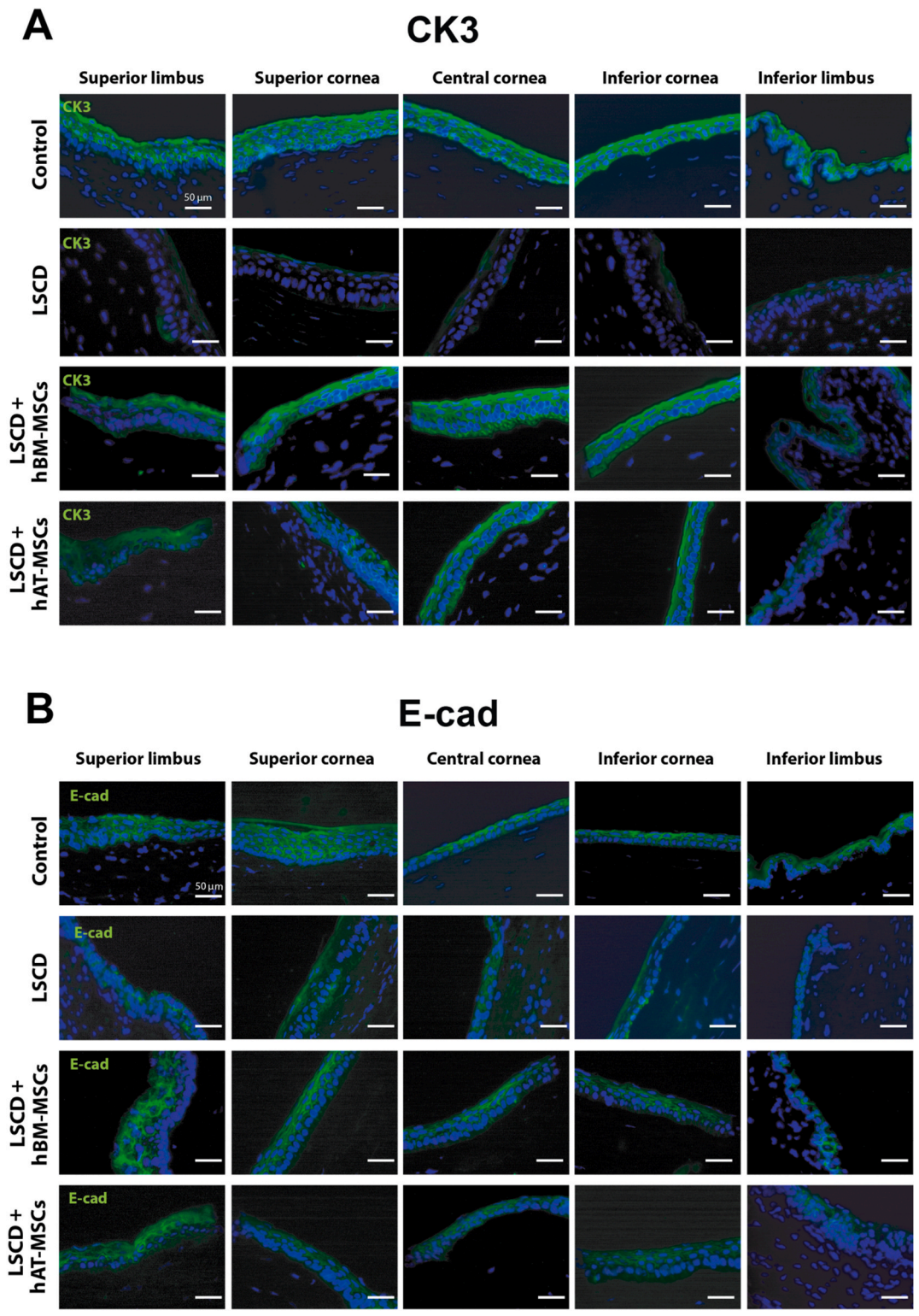

Fig. 5. Immunofluorescence staining of corneal epithelial markers in histological sections. **A** Cytokeratin 3 (CK3). **B** E-cadherin (E-cad). Representative immunofluorescence CK3 and E-cad images in the superior limbus, superior, central and inferior cornea, and inferior limbus in healthy control eyes and at 11 weeks after LSCD induction (8 weeks after hBM-MSC or hAT-MSC transplantation). LSCD eyes with no treatment, LSCD + hBM-MSC eyes, and LSCD + hAT-MSC eyes. Nuclei were counterstained with Hoechst (blue). Scale bar = 50 µm. LSCD: limbal stem cell deficiency; hBM-MSCs: human bone marrow-derived mesenchymal stem cells; hAT-MSCs: human adipose tissue-derived mesenchymal stem cells. (For interpretation of the references to color in this figure legend, the reader is referred to the Web version of this article.)

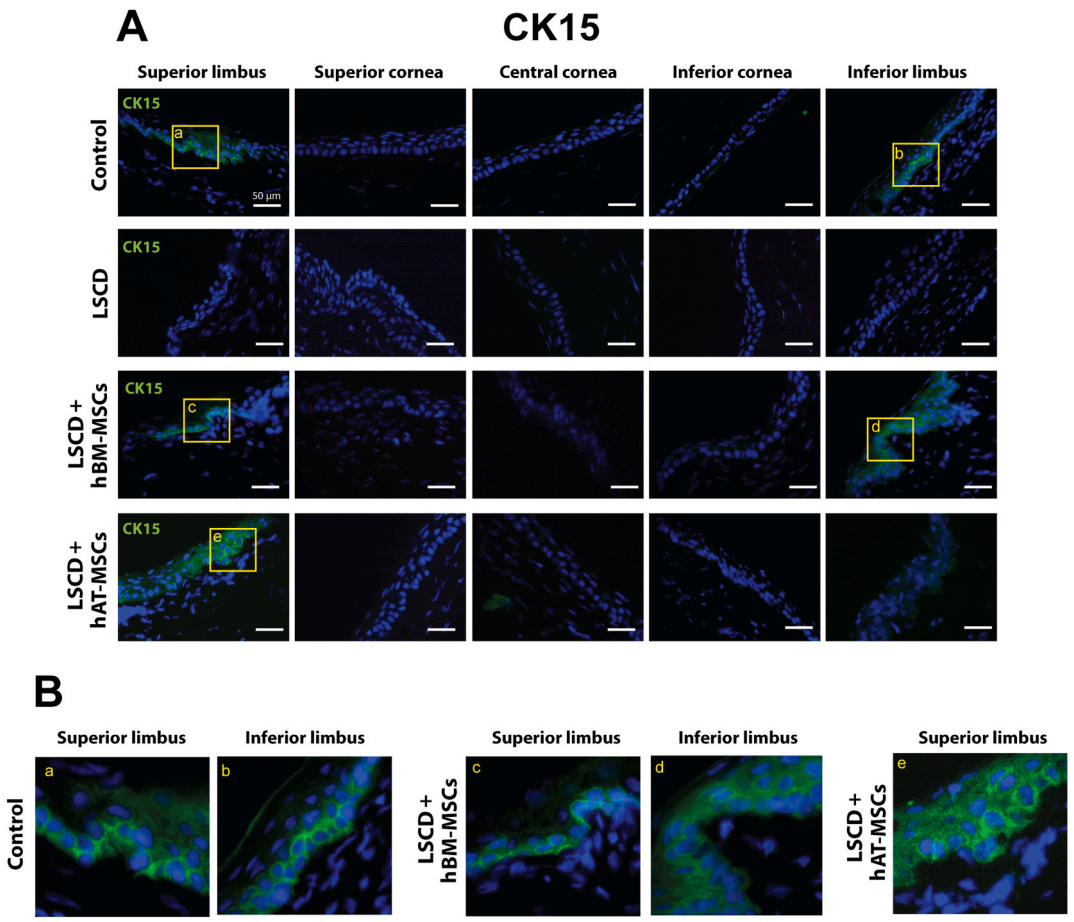

Fig. 6. Immunofluorescence staining of cytokeratin 15 (CK15) as a marker of limbal epithelial stem cells in histological sections. **A** Representative immunofluorescence CK15 images in the superior limbus, superior, central and inferior cornea, and inferior limbus in healthy control eyes and at 11 weeks after LSCD induction (8 weeks after hBM-MSC or hAT-MSC transplantation). LSCD eyes with no treatment, LSCD + hBM-MSC eyes, and LSCD + hAT-MSC eyes. **B** Zoomed-in images of the areas indicated in panel A. Nuclei were counterstained with Hoechst (blue). Scale bar = 50 µm. LSCD: limbal stem cell deficiency; hBM-MSC: human bone marrow-derived mesenchymal stem cells; hAT-MSC: human adipose tissue-derived mesenchymal stem cells. (For interpretation of the references to color in this figure legend, the reader is referred to the Web version of this article.)

treated with either hBM-MSCs or hAT-MSCs, the number of corneal epithelial layers increased. However, the presence of blood vessels in the corneal stroma was significantly lower only in the hAT-MSC–treated group. Several research groups have previously reported similar positive effects for rat BM-MSCs (Ghazaryan et al., 2016; Ma et al., 2006; Rohaina et al., 2014) or hAT-MSCs (Espandar et al., 2014) cultured on amniotic membrane and transplanted onto LSCD eyes. In addition, the presence of lymphocytes, a sign of inflammation, was significantly decreased in the cornea only in eyes treated with hAT-MSCs. Treatment with hBM-MSCs also reduced lymphocytic infiltration, but the effect was just short of statistical significance in the cornea. Differences in the level of inflammation could be due to the higher number of hAT-MSCs compared to the hBM-MSCs that were in the corneal stroma. A decrease in ocular surface inflammation was also observed by other authors when rat, rabbit or hBM-MSCs (Cejkova et al., 2013; Ghazaryan et al., 2016; Rohaina et al., 2014) or hAT-MSCs (Espandar et al., 2014; Galindo et al., 2017) cultured on amniotic membrane or other substrates were administered in LSCD-induced rats or rabbits. Additionally, when hBM-MSCs (Rohaina et al., 2014) or rabbit- or hAT-MSCs (Galindo et al., 2017; Venugopal et al., 2020) were cultured on amniotic membrane or a scaffold and transplanted to the ocular surface of LSCD eyes, a decrease of corneal goblet cells occurred in comparison with untreated animals. We found a similar reduction in conjunctival overgrowth onto the limbus and/or cornea in the LSCD + hAT-MSC group.

At 8 weeks after transplantation, there were no significant differences between the hBM- and hAT-MSC groups in the number of corneal epithelial layers or lymphocytes. Moreover, the percentage of samples with corneal stromal blood vessels was significantly lower in the hAT-MSC–treated group compared to the hBM-MSC–treated group. Thus, both treatment groups supported corneal reepithelization after LSCD initiation, but the hAT-MSC transplants more effectively reduced both deep corneal neovascularization and corneal lymphocyte-associated inflammation. Previously, Holan et al. reported that LSCD rabbits treated with rabbit BM-MSCs and AT-MSCs, each loaded onto nanofiber scaffolds, improved corneal re-epithelization, corneal thickness, and reduced neovascularization, although the improvement was significantly better with BM-MSCs than with AT-MSCs (Holan et al., 2015).

The destruction of the corneal epithelium to create LSCD also removes the corneal epithelial marker CK3 (Galindo et al., 2017; Nieto-Miguel et al., 2011). The restoration of the epithelium during the 8-week post-transplant period for both types of hMSCs was accompanied by increased expression of CK3 in the superior, central, and inferior cornea, approaching that in healthy control eyes. Similarly, Bandeira et al. reported that corneal epithelial markers like CK3 were expressed in rat LSCD corneas after transplantation with epithelial-like cells derived from hAT-MSCs (Bandeira et al., 2020). Sharma et al. also observed corneal reepithelization and CK3 expression and in alkali burned-rabbit corneas after transplanting autologous BM-MSCs on temperature responsive membranes (Sharma et al., 2021).

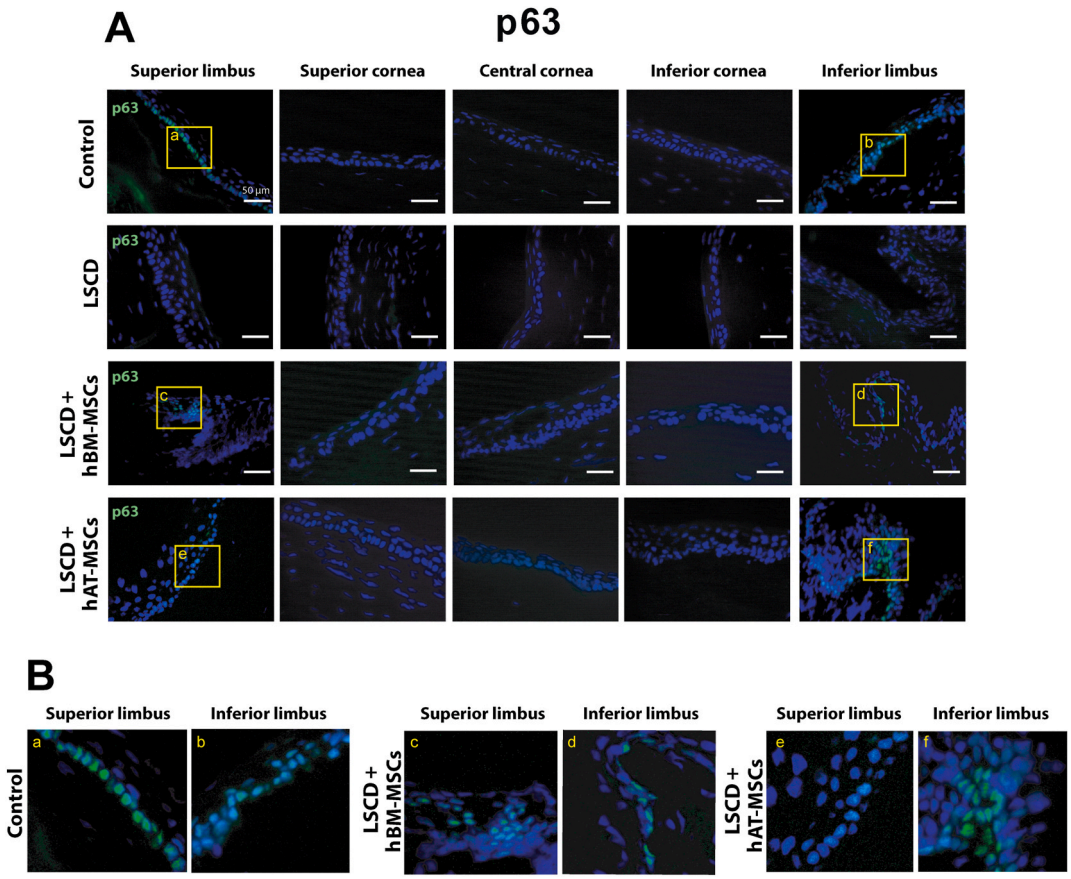

Fig. 7. Immunofluorescence staining of transcription factor p63 (p63) as a marker of limbal epithelial stem cells in histological sections. **A** Representative immunofluorescence p63 images in the superior limbus, superior, central and inferior cornea, and inferior limbus in healthy control eyes and at 11 weeks after LSCD induction (8 weeks after hBM-MSC or hAT-MSC transplantation). LSCD eyes with no treatment, LSCD + hBM-MSC eyes, and LSCD + hAT-MSC eyes. **B** Zoomed-in images of the areas indicated in panel A. Nuclei were counterstained with Hoechst (blue). Scale bar = 50 µm. LSCD: limbal stem cell deficiency; hBM-MSC: human bone marrow-derived mesenchymal stem cells; hAT-MSC: human adipose tissue-derived mesenchymal stem cells. (For interpretation of the references to color in this figure legend, the reader is referred to the Web version of this article.)

We found that expression of the LESC markers CK15 and p63 (Chen et al., 2004; Nieto-Miguel et al., 2011; Pellegrini et al., 2001; Yoshida et al., 2006) was reduced in the LSCD model as previously reported (Galindo et al., 2017). However, both markers increased in the basal layers of the limbal epithelium of LSCD rabbits after transplantation with either hBM-MSC– or hAT-MSC–loaded amniotic membranes. However, p63α expression was not evident in any of the hMSCs cultures, and CK15 was only present in a few hBM-MSCs from one donor. Therefore, the CK15 and p63 expression observed after the transplantation likely came from the differentiation of LESCs from the transplanted hMSCs, or from the recovery of LESCs under the influence of hMSCs trophic factors. These factors would reduce inflammation and neovascularization (Oh et al., 2008), thus providing a microenvironment that would promote the proliferation and differentiation of the remaining resident LESCs.

Khorolskaya et al. recently observed that transplantation of rabbit limbal-MSCs in a rabbit LSCD model stimulates the expression of CK15 not only in the limbal epithelium, but also in the superficial layer of the newly formed corneal epithelium (Khorolskaya et al., 2023). For p63, some authors did not find differences in the expression of p63 after transplantation of autologous BM-MSCs in rabbits with LSCD (Reinshagen et al., 2011). However, other reports agree with our finding of p63 expression recovery after mouse- or hBM-MSC transplantation in mouse and rat models of LSCD, respectively (Lan et al., 2012; Rohaina et al., 2014).

In our study, at 8 weeks after transplantation, BrdU-labeled hBM-MSCs or hAT-MSCs were mostly located in the stroma of the superior limbus. Other labeled cells were sparsely distributed in the epithelia of the superior limbus and the superior and central cornea. Khorolskaya et al. using limbal-MSCs-loaded amniotic membranes found some limbal MSCs within the corneal stroma of LSCD rabbits, as we observed in our study (Khorolskaya et al., 2023).

5. Conclusions

Overall, our results indicate that transplantation to the rabbit ocular surface of hBM-MSCs and hAT-MSCs seeded onto amniotic membrane is safe for rabbits with surgically induced LSCD. Furthermore, this treatment protocol reduces the development of corneal opacity, neovascularization, inflammation, and partially restores the LSCD-damaged

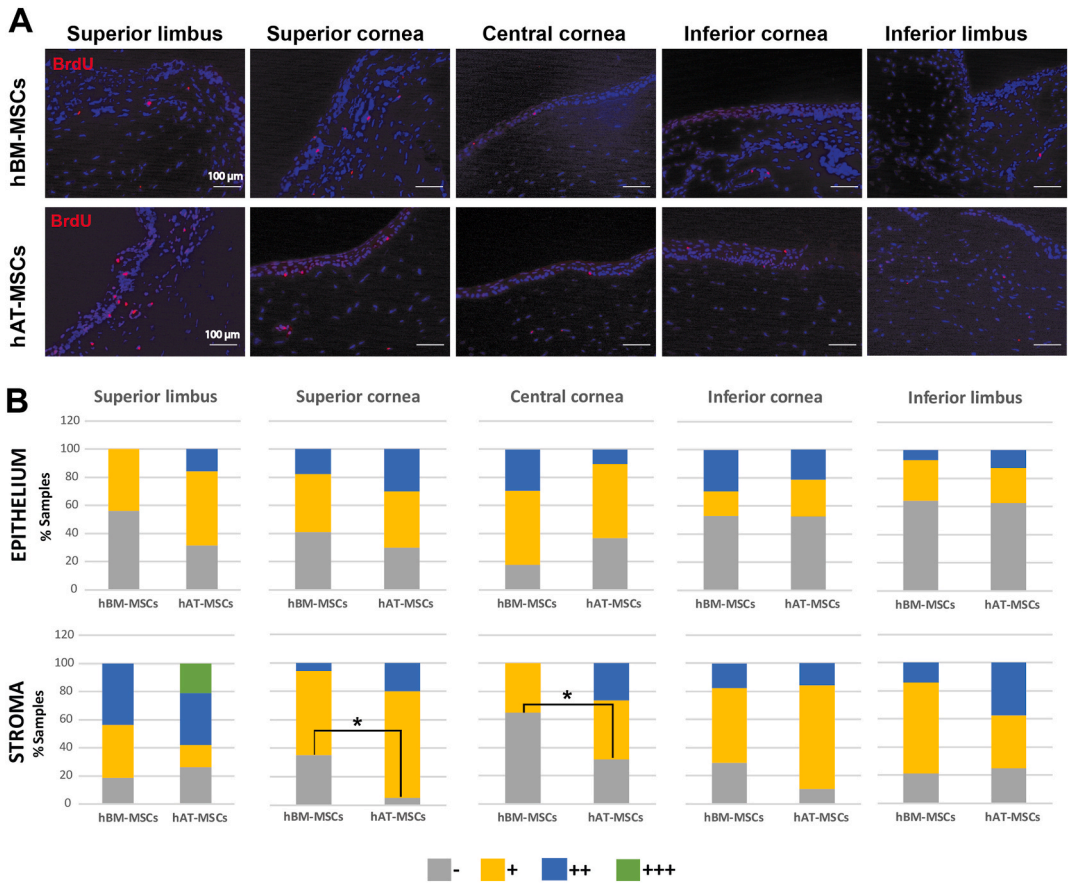

Fig. 8. Immunolocalization of transplanted cells in histological sections at 8 weeks after transplantation. **A** Representative images showing the distribution of BrdU-positive cells (hBM-MSCs and hAT-MSCs) in different ocular surface tissues of transplant-treated LSCD eyes. BrdU (red); nuclei (blue). **B** Percentage of samples with (−) absence of BrdU-positive cells, (+) a few isolated BrdU-positive cells, (++) moderate BrdU-positive cells, and (+++) elevated number of cells. *$p < 0.05$. hBM-MSCs: human bone marrow-derived mesenchymal stem cells; hAT-MSCs: human adipose tissue-derived mesenchymal stem cells; LSCD: limbal stem cell deficiency. (For interpretation of the references to color in this figure legend, the reader is referred to the Web version of this article.)

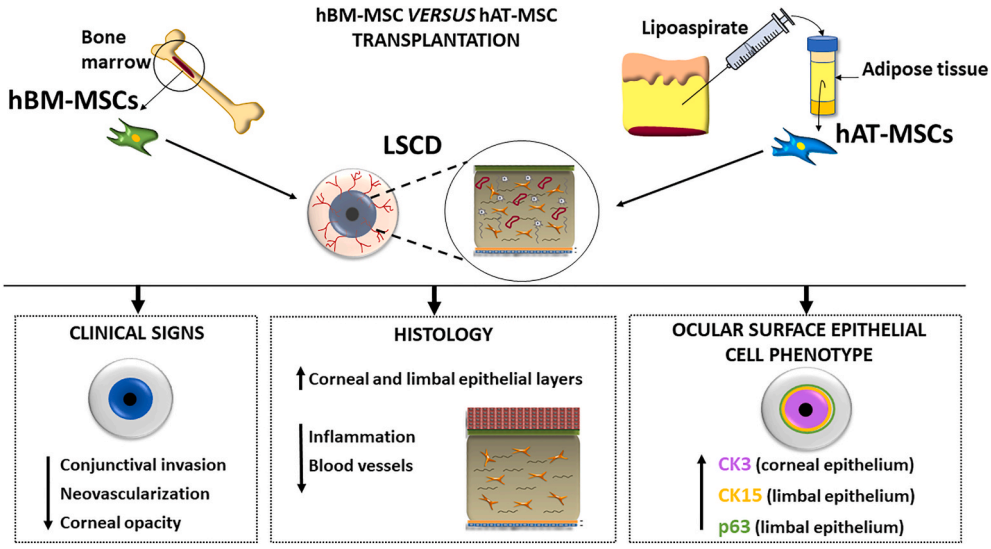

Fig. 9. Comparison of the safety and efficacy of human bone marrow- and adipose tissue-derived mesenchymal stem/stromal cell (hBM-MSC and hAT-MSC) transplantation in an experimental rabbit model of limbal stem cell deficiency (LSCD). Analysis of clinical signs, histology, and ocular surface epithelial cell phenotype. CK3: cytokeratin 3; CK15: cytokeratin 15; p63: nuclear transcription factor p63.

limbal and corneal tissue structure and epithelial cell phenotype (Fig. 9). hAT-MSCs were slightly superior to hBM-MSCs in reducing corneal stromal inflammation. Nevertheless, our results suggest that transplantation of both types of hMSCs now warrants further investigation as valid alternatives to current treatments of patients suffering from corneal failure due to LSCD.

CRediT authorship contribution statement

Sara Galindo: Writing – review & editing, Writing – original draft, Visualization, Methodology, Investigation, Formal analysis, Data curation, Conceptualization. **Marina López-Paniagua:** Writing – review & editing, Writing – original draft, Visualization, Methodology, Investigation, Formal analysis, Data curation, Conceptualization. **Ana de la Mata:** Writing – review & editing, Writing – original draft, Visualization, Methodology, Investigation, Formal analysis, Data curation, Conceptualization. **José M. Herreras:** Writing – review & editing, Methodology, Investigation, Conceptualization. **Carmen García-Vázquez:** Investigation. **Beatriz Marceñido:** Writing – original draft, Visualization, Investigation, Data curation. **Esther Rey:** Investigation. **Celia Higuera-Barón:** Investigation. **Margarita Calonge:** Writing – review & editing, Supervision, Project administration, Methodology, Funding acquisition, Conceptualization. **Teresa Nieto-Miguel:** Writing – review & editing, Writing – original draft, Visualization, Supervision, Project administration, Methodology, Investigation, Funding acquisition, Conceptualization.

Funding statement

This work was supported by: the Ministry of Economy and Competitiveness and the European Regional Development Fund, Spain (Grant SAF2015-63594-R MINECO/FEDER, UE); the Ministry of Science and Innovation, Spain (Grant PID2019-105525RB-100 AEI/10.13039/501100011033); the Carlos III National Institute of Health, CIBER-BBN (CB06/01/003 MICINN/FEDER, UE), Spain; the Department of Education of the Junta de Castilla y León and the European Regional Development Fund (Grant CLU-2023-1-04), and the Centro en Red de Medicina Regenerativa y Terapia Celular de Castilla y León, Spain. The funders had no role in the design of the study; in the collection, analyses, or interpretation of data; in the writing of the manuscript; or in the decision to publish the results.

Conflict of interest

The authors declare that they have no known competing financial interests or personal relationships that could have appeared to influence the work reported in this paper.

Acknowledgements

The authors thank Dr. M. J. Villanueva (Europa Clinic, Valladolid, Spain) for her support in providing human liposuctions and B. Bromberg (Certified Editor in Life Sciences of Xenofile Editing, http://www.xenofileediting.com/) for his assistance in the final editing and preparation of this manuscript. The authors also acknowledge 3datos® (https://www.3datos.es/) for the statistical assistance.

Data availability

Data will be made available on request.

References

Alió del Barrio, J.L., De la Mata, A., De Miguel, M.P., Arnalich-Montiel, F., Nieto-Miguel, T., El Zarif, M., Cadenas-Martín, M., López-Paniagua, M., Galindo, S., Calonge, M., Alió, J.L., 2022. Corneal regeneration using adipose-derived mesenchymal stem cells. Cells 11, 2549. https://doi.org/10.3390/cells11162549.

Bandeira, F., Goh, T.W., Setiawan, M., Yam, G.H.F., Mehta, J.S., 2020. Cellular therapy of corneal epithelial defect by adipose mesenchymal stem cell-derived epithelial progenitors. Stem Cell Res. Ther. 11, 14. https://doi.org/10.1186/s13287-019-1533-1.

Calonge, M., Nieto-Miguel, T., de la Mata, A., Galindo, S., Herreras, J.M., López-Paniagua, M., 2021. Goals and challenges of stem cell-based therapy for corneal blindness due to limbal deficiency. Pharmaceutics 13, 1483. https://doi.org/10.3390/pharmaceutics13091483.

Calonge, M., Pérez, I., Galindo, S., Nieto-Miguel, T., López-Paniagua, M., Fernández, I., Alberca, M., García-Sancho, J., Sánchez, A., Herreras, J.M., 2019. A proof-of-concept clinical trial using mesenchymal stem cells for the treatment of corneal epithelial stem cell deficiency. Transl. Res. 206, 18–40. https://doi.org/10.1016/J.TRSL.2018.11.003.

Cejkova, J., Trosan, P., Cejka, C., Lencova, A., Zajicova, A., Javorkova, E., Kubinova, S., Sykova, E., Holan, V., 2013. Suppression of alkali-induced oxidative injury in the cornea by mesenchymal stem cells growing on nanofiber scaffolds and transferred onto the damaged corneal surface. Exp. Eye Res. 116, 312–323. https://doi.org/10.1016/j.exer.2013.10.002.

Chen, Z., de Paiva, C.S., Luo, L., Kretzer, F.L., Pflugfelder, S.C., Li, D., 2004. Characterization of putative stem cell phenotype in human limbal epithelia. Stem Cell. 22, 355–366. https://doi.org/10.1634/stemcells.22-3-355.

Cotsarelis, G., Cheng, S.Z., Dong, G., Sun, T.T., Lavker, R.M., 1989. Existence of slow-cycling limbal epithelial basal cells that can be preferentially stimulated to proliferate: implications on epithelial stem cells. Cell 57, 201–209. https://doi.org/10.1016/0092-8674(89)90958-6.

Deng, S.X., Borderie, V., Chan, C.C., Dana, R., Figueiredo, F.C., Gomes, J.A.P., Pellegrini, G., Shimmura, S., Kruse, F.E., 2019. Global consensus on definition, classification, diagnosis, and staging of limbal stem cell deficiency. Cornea 38, 364–375. https://doi.org/10.1097/ICO.0000000000001820.

Dominici, M., Le Blanc, K., Mueller, I., Slaper-Cortenbach, I., Marini, F., Krause, D.S., Deans, R.J., Keating, A., Prockop, D.J., Horwitz, E.M., 2006. Minimal criteria for defining multipotent mesenchymal stromal cells. The international society for cellular therapy position statement. Cytotherapy 8, 315–317. https://doi.org/10.1080/14653240600855905.

Dos Santos, A., Balayan, A., Funderburgh, M.L., Ngo, J., Funderburgh, J.L., Deng, S.X., 2019. Differentiation capacity of human mesenchymal stem cells into keratocyte lineage. Investig. Ophthalmol. Vis. Sci. 60, 3013–3023. https://doi.org/10.1167/iovs.19-27008.

Dua, H.S., Saini, J.S., Azuara-Blanco, A., Gupta, P., 2000. Limbal stem cell deficiency: concept, aetiology, clinical presentation, diagnosis and management. Indian J. Ophthalmol. 48, 83–92.

Espandar, L., Caldwell, D., Watson, R., Blanco-Mezquita, T., Zhang, S., Bunnell, B., 2014. Application of adipose-derived stem cells on scleral contact lens carrier in an animal model of severe acute alkaline burn. Eye Contact Lens 40, 243–247. https://doi.org/10.1097/ICL.0000000000000045.

Galindo, S., de la Mata, A., López-Paniagua, M., Herreras, J.M., Pérez, I., Calonge, M., Nieto-Miguel, T., 2021. Subconjunctival injection of mesenchymal stem cells for corneal failure due to limbal stem cell deficiency: state of the art. Stem Cell Res. Ther. 12, 60. https://doi.org/10.1186/s13287-020-02129-0.

Galindo, S., Herreras, J.M., López-Paniagua, M., Rey, E., de la Mata, A., Plata-Cordero, M., Calonge, M., Nieto-Miguel, T., 2017. Therapeutic effect of human adipose tissue-derived mesenchymal stem cells in experimental corneal failure due to limbal stem cell niche damage. Stem Cell. 35, 2160–2174. https://doi.org/10.1002/stem.2672.

Ghazaryan, E., Zhang, Y., He, Y., Liu, X., Li, Y., Xie, J., Su, G., 2016. Mesenchymal stem cells in corneal neovascularization: Comparison of different application routes. Mol. Med. Rep. 14, 3104–3112. https://doi.org/10.3892/mmr.2016.5621.

Ghiasi, M., Jadidi, K., Hashemi, M., Zare, H., Salimi, A., Aghamollaei, H., 2021. Application of mesenchymal stem cells in corneal regeneration. Tissue Cell 73, 101600. https://doi.org/10.1016/j.tice.2021.101600.

Holan, V., Trosan, P., Cejka, C., Javorkova, E., Zajicova, A., Hermankova, B., Chudickova, M., Cejkova, J., 2015. A comparative study of the therapeutic potential of mesenchymal stem cells and limbal epithelial stem cells for ocular surface reconstruction. Stem Cells Transl. Med. 4, 1052–1063. https://doi.org/10.5966/sctm.2015-0039.

Jiang, T.-S., Cai, L., Ji, W.-Y., Hui, Y.-N., Wang, Y.-S., Hu, D., Zhu, J., 2010. Reconstruction of the corneal epithelium with induced marrow mesenchymal stem cells in rats. Mol. Vis. 16, 1304–1316, 144 [pii].

Khorolskaya, J.I., Perepletchikova, D.A., Zhurenkov, K.E., Kachkin, D.V., Rubel, A.A., Blinova, M.I., Mikhailova, N.A., 2023. Corneal reconstruction with EGFP-labelled limbal mesenchymal stem cells in a rabbit model of limbal stem cell deficiency. Int. J. Mol. Sci. 24, 5431. https://doi.org/10.3390/ijms24065431.

Lan, Y., Kodati, S., Lee, H.S., Omoto, M., Jin, Y., Chauhan, S.K., 2012. Kinetics and function of mesenchymal stem cells in corneal injury. Investig. Opthalmol. Vis. Sci. 53, 3638. https://doi.org/10.1167/iovs.11-9311.

Lee, R.H., Yu, J.M., Foskett, A.M., Peltier, G., Reneau, J.C., Bazhanov, N., Oh, J.Y., Prockop, D.J., 2014. TSG-6 as a biomarker to predict efficacy of human mesenchymal stem/progenitor cells (hMSCs) in modulating sterile inflammation in vivo. Proc. Natl. Acad. Sci. 111, 16766–16771. https://doi.org/10.1073/pnas.1416121111.

Lin, H.-F., Lai, Y.-C., Tai, C.-F., Tsai, J.-L., Hsu, H.-C., Hsu, R.-F., Lu, S.-N., Feng, N.-H., Chai, C.-Y., Lee, C.-H., 2013. Effects of cultured human adipose-derived stem cells transplantation on rabbit cornea regeneration after alkaline chemical burn. Kaohsiung J. Med. Sci. 29, 14–18. https://doi.org/10.1016/j.kjms.2012.08.002.

Luetzkendorf, J., Nerger, K., Hering, J., Moegel, A., Hoffmann, K., Hoefers, C., Mueller-Tidow, C., Mueller, L.P., 2015. Cryopreservation does not alter main characteristics of good manufacturing Process–grade human multipotent mesenchymal stromal cells including immunomodulating potential and lack of malignant transformation. Cytotherapy 17, 186–198. https://doi.org/10.1016/j.jcyt.2014.10.018.

Ma, Y., Xu, Y., Xiao, Z., Yang, W., Zhang, C., Song, E., Du, Y., Li, L., 2006. Reconstruction of chemically burned rat corneal surface by bone marrow-derived human mesenchymal stem cells. Stem Cell. 24, 315–321. https://doi.org/10.1634/stemcells.2005-0046.

Martínez-Conesa, E.M., Espel, E., Reina, M., Casaroli-Marano, R.P., 2012. Characterization of ocular surface epithelial and progenitor cell markers in human adipose stromal cells derived from lipoaspirates. Investig. Ophthalmol. Vis. Sci. 53, 513–520. https://doi.org/10.1167/iovs.11-7550.

Nieto-Miguel, T., Calonge, M., de la Mata, A., López-Paniagua, M., Galindo, S., de la Paz, M.F., Corrales, R.M., 2011. A comparison of stem cell-related gene expression in the progenitor-rich limbal epithelium and the differentiating central corneal epithelium. Mol. Vis. 17, 2102–2117.

Nieto-Miguel, T., Galindo, S., López-Paniagua, M., Pérez, I., Herreras, J.M., Calonge, M., 2019. Cell therapy using extraocular mesenchymal stem cells. In: Alió, J., Alió del Barrio, J., Arnalich-Montiel, F. (Eds.), Corneal Regeneration . Essentials in Ophthalmology. Springer, Cham, pp. 231–262. https://doi.org/10.1007/978-3-030-01304-2_17.

Nieto-Miguel, T., Galindo, S., Reinoso, R., Corell, A., Martino, M., Pérez-Simón, J.A., Calonge, M., 2013. In vitro simulation of corneal epithelium microenvironment induces a corneal epithelial-like cell phenotype from human adipose tissue mesenchymal stem cells. Curr. Eye Res. 38, 933–944. https://doi.org/10.3109/02713683.2013.802809.

Nieto-Nicolau, N., Martín-Antonio, B., Müller-Sánchez, C., Casaroli-Marano, R.P., 2020. In vitro potential of human mesenchymal stem cells for corneal epithelial regeneration. Regen. Med 15, 1409–1426. https://doi.org/10.2217/rme-2019-0067.

O'Callaghan, A.R., Daniels, J.T., 2011. Concise review: limbal epithelial stem cell therapy: controversies and challenges. Stem Cell. 29, 1923–1932. https://doi.org/10.1002/stem.756.

Oh, J.Y., Kim, M.K., Shin, M.S., Lee, H.J., Ko, J.H., Wee, W.R., Lee, J.H., 2008. The anti-inflammatory and anti-angiogenic role of mesenchymal stem cells in corneal wound healing following chemical injury. Stem Cell. 26, 1047–1055. https://doi.org/10.1634/stemcells.2007-0737.

Pellegrini, G., Dellambra, E., Golisano, O., Martinelli, E., Fantozzi, I., Bondanza, S., Ponzin, D., McKeon, F., De Luca, M., 2001. p63 identifies keratinocyte stem cells. Proc. Natl. Acad. Sci. 98, 3156–3161. https://doi.org/10.1073/pnas.061032098.

Percie du Sert, N., Hurst, V., Ahluwalia, A., Alam, S., Avey, M.T., Baker, M., Browne, W. J., Clark, A., Cuthill, I.C., Dirnagl, U., Emerson, M., Garner, P., Holgate, S.T., Howells, D.W., Karp, N.A., Lazic, S.E., Lidster, K., MacCallum, C.J., Macleod, M., Pearl, E.J., Petersen, O.H., Rawle, F., Reynolds, P., Rooney, K., Sena, E.S., Silberberg, S.D., Steckler, T., Würbel, H., 2020. The ARRIVE guidelines 2.0: updated guidelines for reporting animal research. PLoS Biol. 18, e3000410. https://doi.org/10.1371/journal.pbio.3000410.

Pınarlı, F.A., Okten, G., Beden, U., Fışgın, T., Kefeli, M., Kara, N., Duru, F., Tomak, L., 2014. Keratinocyte growth factor-2 and autologous serum potentiate the regenerative effect of mesenchymal stem cells in cornea damage in rats. Int. J. Ophthalmol. 7, 211–219. https://doi.org/10.3980/j.issn.2222-3959.2014.02.05.

Rama, P., Matuska, S., Paganoni, G., Spinelli, A., De Luca, M., Pellegrini, G., 2010. Limbal stem-cell therapy and long-term corneal regeneration. N. Engl. J. Med. 363, 147–155. https://doi.org/10.1056/NEJMoa0905955.

Ramírez, B.E., Sánchez, A., Herreras, J.M., Fernández, I., García-Sancho, J., Nieto-Miguel, T., Calonge, M., 2015. Stem cell therapy for corneal epithelium regeneration following good manufacturing and clinical procedures. BioMed Res. Int. 2015, 408495. https://doi.org/10.1155/2015/408495.

Reinshagen, H., Auw-Haedrich, C., Sorg, R.V., Boehringer, D., Eberwein, P., Schwartzkopff, J., Sundmacher, R., Reinhard, T., 2011. Corneal surface reconstruction using adult mesenchymal stem cells in experimental limbal stem cell deficiency in rabbits. Acta Ophthalmol. 89, 741–748. https://doi.org/10.1111/j.1755-3768.2009.01812.x.

Roddy, G.W., Oh, J.Y., Lee, R.H., Bartosh, T.J., Ylostalo, J., Coble, K., Rosa, R.H., Prockop, D.J., 2011. Action at a distance: systemically administered adult stem/progenitor cells (MSCs) reduce inflammatory damage to the cornea without engraftment and primarily by secretion of TNF-α stimulated gene/protein 6. Stem Cell. 29, 1572–1579. https://doi.org/10.1002/stem.708.

Rohaina, C.M., Then, K.Y., Ng, A.M.H., Wan Abdul Halim, W.H., Zahidin, A.Z.M., Saim, A., Idrus, R.B.H., 2014. Reconstruction of limbal stem cell deficient corneal surface with induced human bone marrow mesenchymal stem cells on amniotic membrane. Transl. Res. 163, 200–210. https://doi.org/10.1016/j.trsl.2013.11.004.

Rohban, R., Pieber, T.R., 2017. Mesenchymal stem and progenitor cells in regeneration: tissue specificity and regenerative potential. Stem Cell. Int. 1–16. https://doi.org/10.1155/2017/5173732, 2017.

Schermer, A., Galvin, S., Sun, T.T., 1986. Differentiation-related expression of a major 64K corneal keratin in vivo and in culture suggests limbal location of corneal epithelial stem cells. J. Cell Biol. 103, 49–62. https://doi.org/10.1083/jcb.103.1.49.

Sharma, J., Sharma, R.K., Gupta, P., Gupta, N., Singh, N., 2021. Corneal reconstruction in chemically damaged cornea using temperature responsive surface assisted mesenchymal stem cell transplantation in rabbits. Graefe's Arch. Clin. Exp. Ophthalmol. 259, 1859–1870. https://doi.org/10.1007/s00417-021-05132-0.

Sikora, B., Skubis-Sikora, A., Kimsa-Furdzik, M., Ciszek, W., Kostrzewski, M., Stojko, J., Mazurek, U., Gola, J., 2019. Adipose-derived stem cells undergo differentiation after co-culture with porcine limbal epithelial stem cells. Stem Cell Res. 41, 101609. https://doi.org/10.1016/j.scr.2019.101609.

Strioga, M., Viswanathan, S., Darinskas, A., Slaby, O., Michalek, J., 2012. Same or not the same? Comparison of adipose tissue-derived versus bone marrow-derived mesenchymal stem and stromal cells. Stem Cell. Dev. 21, 2724–2752. https://doi.org/10.1089/scd.2011.0722.

Venkatakrishnan, J., Saeed, Y., Kao, W.W.-Y., 2022. Trends in using mesenchymal stromal/stem cells (MSCs) in treating corneal diseases. Ocul. Surf. 26, 255–267. https://doi.org/10.1016/j.jtos.2022.10.003.

Venugopal, B., Shenoy, S.J., Mohan, S., Anil Kumar, P.R., Kumary, T.V., 2020. Bioengineered corneal epithelial cell sheet from mesenchymal stem cells-A functional alternative to limbal stem cells for ocular surface reconstruction. J. Biomed. Mater. Res. B Appl. Biomater. 108, 1033–1045. https://doi.org/10.1002/jbm.b.34455.

Wan, P., Wang, X., Ma, P., Gao, N., Ge, J., Mou, Y., Wang, Z., 2011. Cell delivery with fixed amniotic membrane reconstructs corneal epithelium in rabbits with limbal stem cell deficiency. Investig. Ophthalmol. Vis. Sci. 52, 724–730. https://doi.org/10.1167/iovs.10-5291.

Yoshida, S., Shimmura, S., Kawakita, T., Miyashita, H., Den, S., Shimazaki, J., Tsubota, K., 2006. Cytokeratin 15 can be used to identify the limbal phenotype in normal and diseased ocular surfaces. Investig. Ophthalmol. Vis. Sci. 47, 4780–4786. https://doi.org/10.1167/iovs.06-0574.

Yun, Y.I., Park, S.Y., Lee, H.J., Ko, J.H., Kim, M.K., Wee, W.R., Reger, R.L., Gregory, C.A., Choi, H., Fulcher, S.F., Prockop, D.J., Oh, J.Y., 2017. Comparison of the anti-inflammatory effects of induced pluripotent stem cell–derived and bone marrow–derived mesenchymal stromal cells in a murine model of corneal injury. Cytotherapy 19, 28–35. https://doi.org/10.1016/j.jcyt.2016.10.007.

Zeppieri, M., Salvetat, M.L., Beltrami, A.P., Cesselli, D., Bergamin, N., Russo, R., Cavaliere, F., Varano, G.P., Alcalde, I., Merayo, J., Brusini, P., Beltrami, C.A., Parodi, P.C., 2013. Human adipose-derived stem cells for the treatment of chemically burned rat cornea: preliminary results. Curr. Eye Res. 38, 451–463. https://doi.org/10.3109/02713683.2012.763100.

Zhang, L., Coulson-Thomas, V.J., Ferreira, T.G., Kao, W.W.Y., 2015. Mesenchymal stem cells for treating ocular surface diseases. BMC Ophthalmol. 15, 155. https://doi.org/10.1186/s12886-015-0138-4.